Biomacromolecules

ARTICLE

pubs.acs.org/Biomac

Three-Dimensional Spatial Patterning of Proteins in Hydrogels

Ryan G. Wylie[†] and Molly S. Shoichet[*,†,‡,§]

[†]Department of Chemistry, University of Toronto, 80 St. George Street, Toronto, ON, Canada M5S 3H6

[‡]Department of Chemical Engineering and Applied Chemistry, University of Toronto, 200 College Street, Toronto, ON, Canada M5S 3E5

[§]Institute of Biomaterials and Biomedical Engineering, 164 College Street, Room 407, Toronto, ON, Canada M5S 3G9

ABSTRACT: The ability to create three-dimensional biochemical environments that mimic those in vivo is valuable for the elucidation of fundamental biological phenomena and pathways. To this end, we designed a system in which proteins can be photochemically patterned in three dimensions within hydrogels under physiological conditions. Fibroblast growth factor-2 (FGF2) was immobilized within agarose hydrogels that were modified with two-photon labile 6-bromo-7-hydroxycoumarin-protected thiols. Two different methods were developed for FGF2 immobilization. The first procedure relies on the protein containing free cysteines for the formation of disulfide bonds with photoexposed agarose thiols. The second procedure takes advantage of the femtomolar binding partners, human serum albumin (HSA) and albumin binding domain (ABD), which have K_D values of $\sim 10^{-14}$ M. Here HSA-maleimide was chemically bound to photoexposed agarose thiols, and then the FGF2-ABD fusion protein was added to form a stable complex with the immobilized HSA. The use of orthogonal, physical binding pairs allows protein immobilization under mild conditions and can be broadly applied to any protein expressed as an ABD fusion.

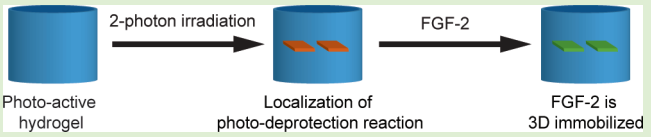

INTRODUCTION

The development of techniques for synthesizing matrices mimicking the three-dimensional (3D) signaling environment in vivo is key to accurately elucidating cellular activities.[1] Although many important findings have been and will continue to be discovered using two-dimensional (2D) cultures systems, many cellular functions are influenced by the spatial arrangement of the 3D microenvironment (those provided by other cells, the extracellular matrix proteins, presentation of growth factors, mechanical properties, etc.[2]) that cannot be adequately represented in a 2D system. Hydrogels have proven to be useful substrates for studying biochemical cues that depend on the 3D environment;[1,3,4] however, current hydrogels lack the chemical complexity required to mimic in vivo environments. To address these limitations, researchers have been developing 3D patterning systems for biomolecules. The majority of the work has focused on the immobilization of adhesive peptides within hydrogels to influence cell migration and morphology.[5,6] Current research is focused on the development of methods for protein immobilization for more complex studies, such as vascular endothelial growth factor (VEGF) gradients to encourage vascularization.[7] The creation of protein patterns in complex and versatile systems needs to be developed for 3D protein immobilization. Patterning technologies will be useful tools for 3D cell culture to improve our understanding of cellular behavior in vivo.

Hydrogels are commonly used as 3D scaffolds because they can be designed to mimic the extracellular matrix (ECM) both chemically and physically.[1] Natural hydrogels made from components of the ECM, such as collagen, elastin, and fibrin, are frequently used because they are intrinsically biocompatible. Furthermore, these hydrogels contain bioactive elements such as adhesion sites, which can promote cell survival and proliferation.[1,8] However, hydrogels with natural bioactive sites are not optimal for patterning experiments because they contain intrinsic biological signals. For example, specific adhesion sites cannot be patterned into collagen hydrogels because they are already highly cell adhesive. The optimal hydrogel would be a blank canvas on which biochemical signals can be incorporated in three dimensions through biomolecule immobilization. Natural hydrogels, from nonmammalian sources such as alginate and agarose, and synthetic hydrogels, such as polyethylene glycol (PEG) and poly(*N*-isopropyl acrylamide) (poly-NIPAAM), are biochemically inert and thus provide an ideal blank canvas for biochemical patterning.

Proteoglycan-binding proteins, such as fibroblast growth factor-2 (FGF2), are particularly amenable to immobilization strategies because they are presented by the ECM.[9] Proteoglycans are heavily glycosylated proteins that form part of the insoluble matrix of the ECM and contain binding sites for many growth factors and cytokines. For example, heparin sulfate proteoglycans have been shown to sequester growth factors both for the establishment of reservoirs and for the creation of spatial gradients.[10,11] Interestingly, many proteins are presented to cells from the ECM as bound ligands, thereby providing a rationale for our protein immobilization strategy.[11] FGF2 was chosen as a model protein for immobilization because it naturally exists as an immobilized signaling molecule[11] and is implicated in many cellular processes, including differentiation,[12] regeneration,[13] wound repair,[14]

Received: July 26, 2011
Revised: August 17, 2011
Published: August 19, 2011

dx.doi.org/10.1021/bm201037j | *Biomacromolecules* 2011, 12, 3789–3796

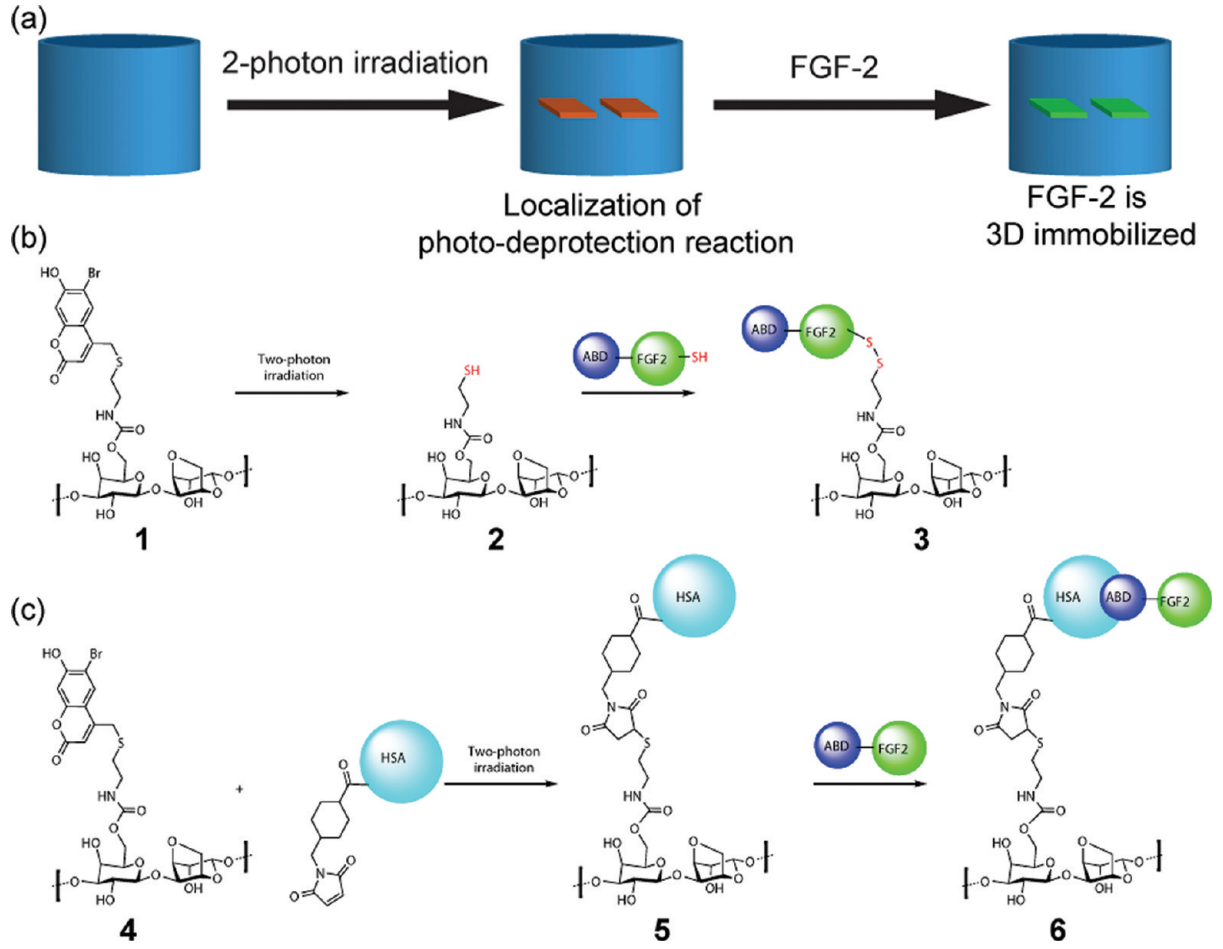

Figure 1. 3D immobilization of FGF2-ABD to agarose through either disulfide bonds or HSA and ABD protein binding pairs. (a) Schematic diagram demonstrating the 3D photodeprotection of thiols in agarose-thiol-Bhc gels for the coupling of FGF2. (b) FGF2-ABD was immobilized to agarose-thiol through disulfides bonds. Thiols are deprotected by two-photon excitation of coumarin (740 nm), which subsequently forms disulfide bonds with free cysteines on FGF2-ABD. (c) FGF2-ABD was immobilized using the physical binding pair of HSA and ABD. Maleimide-HSA was immobilized through two-photon irradiation of agarose as in panel b, followed by the addition of FGF2-ABD, which selectively binds with immobilized HSA.

and vascularization.[15,16] Immobilized FGF2 has also been shown to promote several cellular activities, including proliferation,[17] migration,[18] and cell organization.[9] Because of this breadth of activity, 3D patterns of FGF2 could have wide applicability in the elucidation of biological pathways and phenomena.

A number of photochemical methods have been utilized to achieve 3D patterns of proteins in hydrogels using either photoinitiators or photocages. For example, the first 3D patterned peptide hydrogel was designed with maleimide-modified peptides that readily reacted with deprotected photocaged thiols in distinct volumes.[5] Thiol-containing biomolecules, such as RGDSC, were patterned into alkene-containing hydrogels using thiol-ene chemistry. In the presence of a photoactive hydrogen-abstracting initiator, thiols are deprotonated to thiyl radicals for reaction with alkenes in the gel.[6,19,20] Acrylate-modified peptides and proteins have also been patterned into hydrogels containing acrylate groups using two-photon active initiators.[21−23] 3D patterns of proteins have already proven useful in tissue engineering. For example, 3D immobilized VEGF encourages tubulogenesis of endothelial cells for the creation of vasculature.[7,24] Moreover, immobilized EphrinA1 also encourages microvascularization, further solidifying the rationale for immobilized proteins in tissue engineering.[25]

We designed a system that achieves 3D immobilization of proteins without the need for a chemical cross-linker within transparent hydrogels, which could prove advantageous in the preservation of bioactivity. This system could then be used to study cellular processes or as a tool in tissue engineering to guide cell fate in three dimensions. To this end, FGF2 was immobilized within agarose hydrogels using two-photon chemistry, which provides the necessary 3D control because the excitation and thus the reaction volume are limited to the focal point of the laser.[26] Agarose was modified with 6-bromo-7-hydroxycoumarin (Bhc)-protected thiols, which are deprotected upon excitation to yield reactive thiols and were subsequently used for the immobilization of proteins (Figure 1). Bhc was chosen as the photocage over more common cages such as 2-nitrobenzyl because Bhc has a larger two-photon uncaging cross section,[27] thus increasing the yield of the photouncaging. Bhc has previously been used in cell culture experiments without any measurable toxicity.[7,27] FGF2 was immobilized through either disulfide bonds or the strong physical interaction between human serum albumin (HSA) and the albumin binding domain (ABD) (Figure 1). Immobilization of proteins using disulfide bonds has previously been established as an efficient method.[28] Strong physical interactions

have also been shown to be stable and useful for protein immobilization.[29]

EXPERIMENTAL SECTION

Materials. *Escherichia coli* BL21(DE3) was purchased from New England Biolabs (Ipswich, MA). Isopropyl β-D-1-thiogalactopyranoside, ampicillin, and terrific broth were purchased from Bioshop Canada Inc. (Burlington, ON). Mouse fibroblast growth factor-2, human serum albumin (fatty acid free), and anti-foam 204 were purchased from Sigma-Aldrich (Oakville, ON). Ni-NTA agarose was purchased from Qiagen (Valencia, CA). Sulfosuccinimidyl-4-(*N*-maleimidomethyl)cyclohexane-1-carboxylate was purchased from Thermo Scientific (Waltman, MA). Alexa Fluor 546 C_5 maleimide was purchased from Invitrogen (Carlsbad, CA). The plasmid encoding FGF2-ABD in pET-21a(+) was purchased from Genscript (Piscataway, NJ).

Methods. *Preparation of Agarose-Thiol-Bhc Gels.* Coumarin-sulfide agarose was prepared as previously reported with minor modifications.[30] Agarose (400 mg) in 40 mL of DMSO was mixed with 180 mg of carbonyl diimidazole for 2 h, followed by the addition of 100 mg of coumarin sulfide with 5 drops of triethylamine. After 24 h, the product was purified by dialysis against water, yielding a substitution rate of 2.8% (i.e., 2.8% of the agarose repeat units were modified with thiol-Bhc). Gels were formed in chambers comprised of o-rings (outer diameter, 0.7 mm; inner diameter, 0.5 mm; and height, 0.2 mm) attached to coverslips.

Expression and Purification of FGF2-ABD. A pET-21a(+) plasmid (Novagen) encoding a fusion protein of mouse FGF2 and a modified ABD[31] with a six-histidine tag for Ni-NTA purification was transformed into chemically competent *E. coli* BL21(DE3). Protein expression was conducted in a 1.8 L culture consisting of 85.7 g of terrific broth, 14.4 mL of glycerol, 6 drops of anti-foam 204, and 180 mg of ampicillin. *E. coli* was grown at 37 °C with air sparging until an OD_{600} of 0.8 was reached, followed by the addition of 342 mg of isopropyl β-D-1-thiogalactopyranoside (IPTG) while the temperature was lowered to 16 °C. After 20 h, the cells were pelleted by centrifugation at 12227*g* for 10 min (Beckman coulter centrifuge Avanti J-26 with rotor JLA-8.1000), resuspended in 60 mL of buffer [50 mM Tris (pH 7.5), 500 mM NaCl, and 5 mM imidazole], and sonicated for 10 min at 30% amplitude with a pulse of 2 s (Misonix S-4000 Sonicator Ultrasonic Processor equipped with a Dual Horn probe). The slurry was centrifuged at 45000*g* for 15 min at 4 °C (Beckman Coulter centrifuge Avanti J-26 with rotor JA-25.50). The liquid fraction was incubated with 2 mL of a nickel-nitrilotriacetic acid (Ni-NTA) resin solution for 15 min at 4 °C. The resin was collected in a column with a glass frit, washed 10 times with 10 mL of 50 mM Tris (pH 7.5), 500 mM NaCl, and 30 mM imidazole, and eluted with 50 mM Tris (pH 7.5), 500 mM NaCl, and 250 mM imidazole. The protein solution was then loaded onto a heparin column (HiTrap Heparin HP 1 mL, GE Healthcare, Piscataway, NJ) and further purified over a NaCl gradient from 0 mM to 2 M in phosphate buffer (pH 7.3). Pure protein (2 mg) was obtained after size-exclusion chromatography (SEC) in 10 mM phosphate buffer (pH 7.3) with 250 mM NaCl using fast protein liquid chromatography (FPLC) (Superdex 75 HR 10/30, AKTA Explorer 10, Amersham Pharmacia). Protein concentrations were determined by absorbance at 280 nm using an extinction coefficient of 18490 M^{-1} cm^{-1} and a molecular mass of 27336 Da.

Labeling of FGF2-ABD with Alexa Fluor 546. A solution consisting of 500 μL of 1 mg/mL FGF2-ABD in 10 mM phosphate buffer (pH 7.3) with 250 mM NaCl and 10 μL of 10 mg/mL maleimide Alexa Fluor 546 in DMSO was mixed for 2 h at room temperature. The protein was purified using 200 μL of Ni-NTA resin, washed 10 times with 1 mL of 50 mM Tris (pH 7.5), 500 mM NaCl, and 30 mM imidazole, and eluted in 250 μL of 50 mM Tris (pH 7.5), 500 mM NaCl, and 250 mM imidazole, yielding 220 μg of FGF2-ABD-546. The substitution rate was determined to be 0.61 mol of Alexa Fluor 546/mol of protein calculated according to a method of Invitrogen.[32] Briefly, the absorbance at 546 nm of the protein solution was measured to determine the concentration of Alexa Fluor 546. The protein concentration was then determined using the absorbance at 280 nm, and the absorbance contribution of Alexa Fluor 546 at 280 nm was removed. The concentration of Alexa Fluor 546 was divided by the protein concentration to determine the substitution ratio.

Addition of Maleimide to HSA. A solution consisting of 500 μL of a 5 mg/mL solution of HSA in PBS and 100 μL of 35 mg/mL sulfo-SMCC in DMSO was mixed for 2 h. The protein was purified by SEC (FPLC, Superdex 200 prep grade HiLoad 16/60, AKTA Explorer 10, Amersham Pharmacia) with PBS (pH 6.8) as the running buffer, yielding 2.2 mg of maleimide (mal) HSA. The protein solution was concentrated to 4 mg/mL with a centrifuge (Vivaspin 20 10 kDa, GE Healthcare). Solutions were stored at −80 °C until they were used.

Bioactivity of Recombinant FGF2-ABD. Mouse neural stem progenitor cells (NSPCs) were isolated from the subventricular zone;[33] 5000 cells (passage 2) were plated per well in a 48-well plate in serum free medium (DMEM/F12 with 20 ng/mL EGF and 2 μg/mL heparin) with varying concentrations (0−1.2 nM) of either FGF2-ABD or commercial FGF2. The numbers of neurospheres greater than 100 μm in diameter were counted for each condition after cells had been cultured for 7 days as a measure of bioactivity.

Photopatterning and Imaging. All patterns were created and imaged on a Leica TCS-SP2 confocal microscope equipped with a Green HeNe laser (1.2 mW, 543), a multiphoton Mai Tai laser, a 20× objective (NA = 0.4), and an electronic stage. The multiphoton laser was set to 740 nm with an offset of 75% and gain of 0% for visualization and an offset of 75% and gain of 43% for patterning. The uncaging of thiols can be immediately visualized by the loss of fluorescence from Bhc. Patterns of FGF2-ABD were visualized with the following settings: laser 543 at 100%, wavelengths from 560 to 700 nm collected, photomultiplier tube at 845 V, and six scans on average per image. Leica version 2.5.1227a was used for the visualization and fluorescence quantification.

Patterning FGF2-ABD-SH to Agarose-SH through Disulfide Bonds. Gels with 1 wt % agarose-thiol-Bhc in PBS (pH 6.8, 20 μL) were patterned by selecting a region of interest of 100 μm × 100 μm forming a square 500 μm below the gel. A series of squares was patterned with a varying number of lasers scans (from 5 to 50). After the gels had been washed in PBS (pH 7.4) for 24 h, 100 μL of 0.15 mg/mL FGF2-ABD-546 was placed on top of the gel for 16 h at 4 °C. The gels were the washed for 2 days in 200 mL of PBS (pH 7.4) with daily buffer replacement. Z-Stacks spanning 100 μm in depth were constructed to determine the axial fluorescence profile.

Patterning FGF2-ABD to Agarose-HSA. Twenty microliters of 1 wt % agarose-thiol-Bhc with 2 mg/mL mal-HSA in PBS (pH 6.8) was irradiated in the same manner described above. After excess mal-HSA had been removed by soaking the gels in PBS (pH 7.4) with 5 mM β-mercaptoethanol for 1 day, FGF2-ABD-546 was introduced as described above. Therefore, immobilization occurred in PBS buffer at pH 7.4 with 1 mM β-mercaptoethanol, thereby ensuring only agarose-HSA would react with FGF2-ABD.

Testing the Stability of the FGF2-ABD Pattern with HSA. The fluorescence intensity of 100 μm × 100 μm squares patterned with 50 scans of two-photon exposure was followed over 8 days in PBS with and without soluble HSA. Gels were soaked in either 30 mL of PBS or 30 mL of PBS with 10 mg/mL HSA. The fluorescence intensity of the patterns was measured on days 0, 2, 5, and 8. Changes in fluorescence were compared by normalizing to day 0.

Quantification of FGF2-ABD. To convert the fluorescence intensity into protein concentration, a calibration curve was constructed for Alexa Fluor 546. A 1 wt % agarose-thiol-Bhc hydrogel with concentrations of 0, 5.75, 11.5, 23, 29, 45, 70, and 110 nM was imaged 500 μm below the surface of the gel. The calibration curve along with the known number of

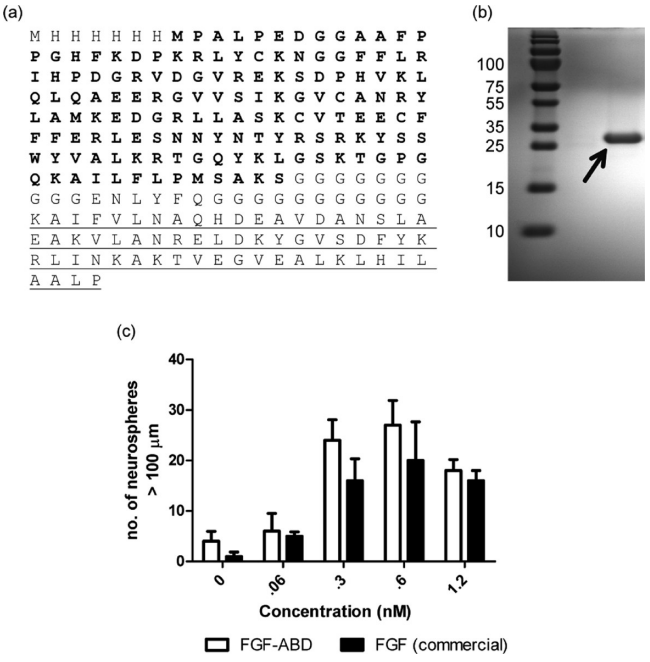

Figure 2. Expression, purification, and bioactivity of FGF2-ABD. (a) Protein sequence of the expressed FGF2-ABD with FGF2 at the N-terminus (bold) and the ABD at the C-terminus underlined, with a spacer between the two sequences to minimize interdomain interactions. (b) SDS−PAGE protein electrophoresis of purified FGF2-ABD shows that a pure sample (indicated with an arrow) with the proper molecular mass (27336 Da) was expressed. (c) FGF2-ABD was determined to be bioactive by counting the number of neurospheres formed from NSPCs after they had been cultured for 7 days. NSPCs were cultured as single cells in 48-well plates in the presence of varying concentrations of FGF2-ABD or commercial FGF2. The bioactivity of FGF2-ABD was similar to that of commercial FGF2 (mean ± standard deviation shown; $n = 3$ for each condition; one-way ANOVA Tukey's post hoc test, $p < 0.05$).

546 tags per protein was used to calculate the protein concentration for each square.

Statistical Analysis. All statistics were determined using GraphPad Prism 5 (GraphPad, La Jolla, CA). Differences among groups were assessed either by a *t* test or by ANOVA with Tukey's post hoc analysis. All data are presented as means ± the standard deviation.

RESULTS

Synthesis and Characterization of FGF2-ABD and Mal-HSA. In this study, FGF2-ABD was expressed from *E. coli* transformed with a pET-21a(+) plasmid encoding the protein sequence (Figure 2a). To increase the percentage of protein in the soluble fraction, expression was performed at 16 °C. At 37 °C, the majority of the protein remains in the insoluble fraction. After expression and collection of the soluble fraction, the protein was purified using a combination of three columns: (1) Ni-NTA, (2) heparin, and (3) size-exclusion chromatography (SEC). The purity of FGF2-ABD was confirmed by sodium dodecyl sulfate−polyacrylamide gel electrophoresis (SDS−PAGE) (Figure 2b).

We found that recombinantly expressed FGF2-ABD was bioactive by comparison to commercially available FGF2 using the neurosphere assay (Figure 2c). Here, bioactive FGF2 is required for neurosphere formation from NSPCs seeded as

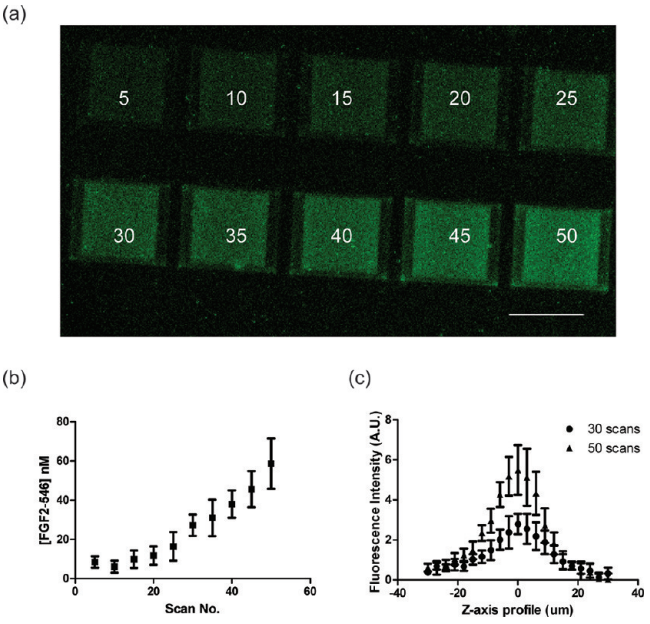

Figure 3. 3D immobilization of FGF2-ABD-546 through disulfide bonds. (a) Confocal micrograph of a series of squares with varying concentrations of FGF2-ABD-546. Ten squares were patterned 500 μm below the surface of the hydrogel with 5−50 laser scans (scale bar, 100 μm). (b) The concentration of FGF2-ABD was quantified by converting the fluorescence intensity of each square using a calibration curve. An FGF2-ABD concentration range from 8.5 ± 2.9 to 58.7 ± 12.9 nM was immobilized (mean ± standard deviation shown; $n = 3$ for each condition). (c) The fluorescence *z*-axis profile of the squares for 30 and 50 scans was measured to determine the axial resolution. A resolution of approximately 40 μm was achieved for each square (mean ± standard deviation shown; $n = 3$ for each condition).

single cells.[33] As the FGF2 concentration increased, so did the number of neurospheres. There was no significant difference in the number of neurospheres between our expressed FGF2-ABD and commercial FGF2 at any concentration (one-way ANOVA Tukey's post hoc test, $p < 0.05$).

Mal-HSA was synthesized by reacting HSA with sulfo-SMCC[34] and purified by SEC. We observed no evidence of protein cross-linking; mal-HSA eluted at the same time as HSA by SEC. The degree of modification was determined by MALDI-TOF; unmodified HSA produced a primary peak of 66524 Da, whereas modified HSA produced a broad peak with an average molar mass of 71071 Da. Given that the addition of a maleimide group would increase the mass by 219 Da, it was calculated that an average of 20.8 maleimides were added per HSA molecule. Because HSA contains 59 lysines,[35] and assuming only lysine primary amines reacted, we estimated that approximately one in three lysines was modified.

Immobilization of FGF2 Using Disulfide Bonds. The 3D localization of FGF2-ABD-546 was successfully achieved by introducing the protein within a two-photon patterned agarose-thiol hydrogel. While the ABD was not necessary for the formation of disulfide bonds, keeping the FGF2-ABD constant across both patterning methodologies allowed us to compare groups. A pattern of squares with different fluorescence intensities was created 500 μm below the surface of the gel (Figure 3a) by raster scanning across a given volume a set number of times. As observed, the fluorescence intensity increased with the number of scans because there were increasing numbers of deprotected

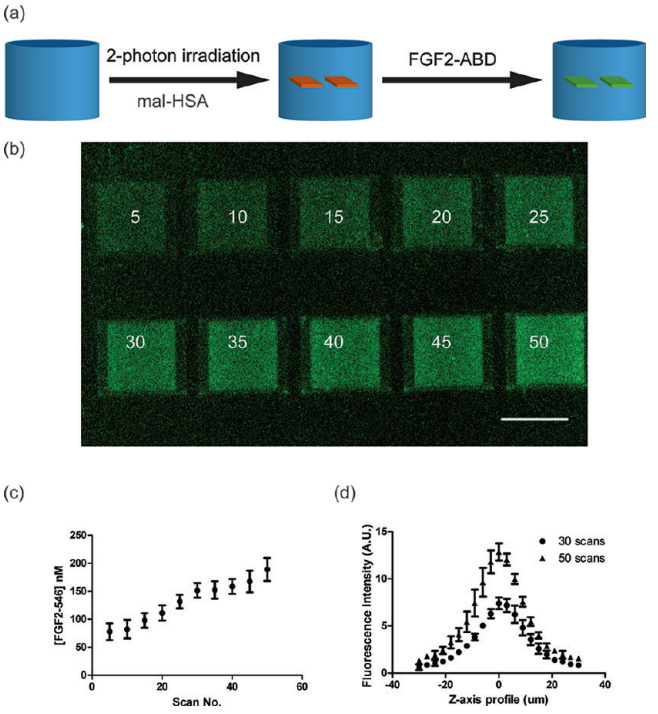

Figure 4. 3D immobilization of FGF2-ABD-546 using the physical binding interaction of HSA and ABD. (a) Scheme for the immobilization of FGF2-ABD by first immobilizing mal-HSA to agarose-thiol using two-photon irradiation. (b) Confocal micrograph of immobilized FGF2-ABD-546 in a series of 10 squares scanned 5−50 times. Fluorescence increased as a function of scan number (scale bar, 100 μm). (c) The concentration of FGF2-ABD was quantified by converting the fluorescence intensity of each square using a calibration curve. An FGF2-ABD concentration range from 77.9 ± 15.1 to 189.1 ± 20.6 nM was immobilized (mean ± standard deviation shown; n = 3 for each condition). (d) The fluorescence z-axis profile was determined for squares scanned 30 and 50 times to determine the axial resolution. A resolution of approximately 40 μm was achieved for each square (mean ± standard deviation shown; n = 3 for each condition).

thiols available to react with FGF2-thiols. A range from 8.5 ± 2.9 to 58.7 ± 12.9 nM was immobilized by increasing the number of laser scans from 5 to 50 (Figure 3b). The axial (z-axis) fluorescence profile of boxes scanned 30 and 50 times was quantified and yielded a Gaussian distribution over a 40 μm depth (Figure 3c). To demonstrate the requirement of thiols for immobilization, we attempted to pattern streptavidin, which does not contain accessible cysteines. No pattern resulted, indicating the necessity of free thiols on the protein for successful immobilization.

Immobilization of FGF2 Using HSA/ABD. The second immobilization strategy with FGF2 took advantage of physical binding partners designed for proteins without disulfide bonds. FGF2-ABD was immobilized by first photopatterning mal-HSA within distinct volumes of Bhc-photocleaved agarose-thiol (Figure 4a). The gel was washed in PBS (pH 7.4) with 5 mM β-mercaptoethanol to quench any unreacted maleimides. FGF2-ABD-546 was then added, followed by a washing step before visualization. Using this method, a series of boxes was created, with the fluorescence intensity increasing with the number of raster scans (Figure 4b). By comparing the fluorescence to a calibration curve, we calculated that FGF2 concentrations ranging from 77.9 ± 15.1 and 189.1 ± 20.6 nM were immobilized by

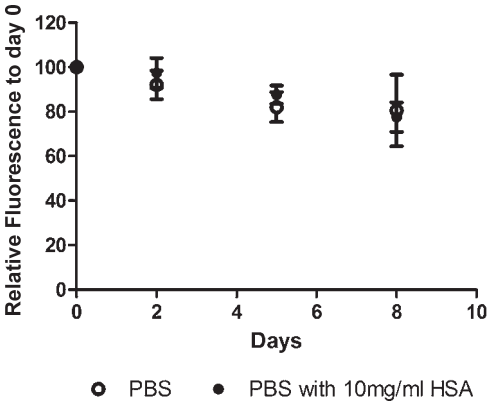

Figure 5. Immobilized FGF2-ABD-546 complexed with HSA is stable in PBS in both the presence and absence of soluble HSA. The fluorescence intensity of the sample having squares scanned 50 times immersed in 30 mL of (○) PBS or (●) PBS with 10 mg/mL HSA was followed over time. No significant difference was observed between the conditions (PBS vs PBS with 10 mg/mL HSA) at any time point, indicating the complex is stable in the presence of soluble HSA (mean ± standard deviation shown; n = 3 for each condition; unpaired t test, p < 0.05). The complex was also determined to be stable over time because no significant difference in fluorescence was observed between any time points for the same condition (ANOVA with Tukey's post hoc analysis, p < 0.05).

increasing the number of laser scans from 5 to 50 (Figure 4c). As we described for the disulfide modification strategy, the fluorescence profile in the z-axis of the squares for 30 and 50 scans showed an axial resolution of approximately 40 μm for the FGF2-ABD/HSA-agarose strategy (Figure 4d).

Stability of the HSA/FGF2-ABD Complex. Given the prevalence of albumin in cell culture media and the fact that the HSA/ABD complex has a noncovalent bond, the stability of the immobilized FGF2-ABD complex with agarose-HSA was investigated in the presence and absence of soluble HSA. The fluorescence intensity was followed over an 8 day period of the samples that had boxes scanned 50 times (Figure 5). With the fluorescence at day 0 set to 100%, the depletion of fluorescence intensity was followed in the presence of 10 mg/mL HSA dissolved in PBS or simply PBS alone. To ensure the stability of the pattern under cell culture conditions, the concentration of soluble HSA (10 mg/mL) used was greater than that commonly found in serum; for example, medium with 10% serum contains ~2 mg/mL albumin.[36] Over the 8 day period, the fluorescence intensity decreased to 80.6 ± 16.1% when the sample was immersed in PBS and to 77.5 ± 6.6% when the sample was immersed in HSA. No significant difference between samples in PBS or 10 mg/mL HSA in PBS at any time point was observed (mean ± standard deviation shown; n = 3 for each condition; unpaired t test, p < 0.05), leading us to conclude that the FGF2-ABD/agarose-HSA interaction is not influenced by the presence of soluble HSA. The decrease in fluorescence over time for both conditions is not statistically significant, indicating that the complex is stable over the time period tested (p < 0.05).

DISCUSSION

The patterning of proteins within two-photon active hydrogels offers a platform for the construction of 3D biomimetic environments for cell culture. In this study, we developed two

methods for the immobilization of FGF2 with agarose-thiol-Bhc: (1) through the formation of disulfide bonds and (2) using the physical interaction between HSA and ABD (Figure 1). For the first strategy, we took advantage of the two free cysteines of FGF2, which are not in the active site and are available to form disulfide bonds with photoexposed agarose-thiol groups.[37,38] For the second strategy, we took advantage of the orthogonal binding between HSA and ABD by first immobilizing maleimide-HSA to photodeprotected thiols by Michael-type addition and then introducing FGF2-ABD as a fusion protein. Both systems allowed FGF2 to be immobilized under mild conditions to maintain bioactivity and can be used as a model for the 3D immobilization of numerous proteins.

Proteins with free cysteines, such as FGF2, can be directly photopatterned in hydrogels with available thiol reactive groups, as we demonstrate here with agarose thiol-Bhc hydrogels in a single step. The concentration of agarose-thiols available to react for protein conjugation is independent of the protein being conjugated and dependent only on the photopatterning.[30] The 3D localization of FGF2-ABD-546, labeled for visualization with Alexa Fluor 546, was successfully achieved by simply introducing the protein within a two-photon patterned agarose-thiol hydrogel. As observed, the immobilized concentration can be tailored for the introduction of gradients, which are useful for cell migration[18] (Figure 3b); 8.5 ± 2.9 nM represents the lowest detectable concentration of FGF2-ABD-546 as visualized with the confocal microscope. Lower concentrations could be quantified using an instrument with greater sensitivity. Because each square was scanned on only one plane, the *z*-axis fluorescence profile represents the axial resolution. In this case, a Gaussian distribution was observed spanning approximately 40 μm. Moreover, immobilization using disulfide bonds can also be applied to proteins without free cysteines by either converting amines into thiols through reaction with Traut's reagent[39] or by the recombinant incorporation of cysteines into the peptide sequence. Therefore, this system is a versatile model for 3D protein immobilization.

Proteins can also be engineered with peptide binding domains, such as ABD, for immobilization. The equilibrium dissociation constant (K_D) for the wild-type sequence of ABD for HSA is only 1.2 nM,[31] similar to those for reversible interactions used for protein purification such as the FLAG tag with an anti-FLAG antibody.[40] Jonsson et al. have engineered a number of ABDs with varying affinities for HSA reaching femtomolar levels,[31] which is necessary to form stable complexes for immobilization experiments. Therefore, we incorporated the ABD sequence with the strongest affinity (or a very low dissociation constant, K_D, of $\sim 10^{-14}$ M) at the C-terminus of FGF2. This interaction has a binding affinity similar to that of biotin-streptavidin, which has been successfully used in protein immobilization studies.[41] A spacer of 28 residues was incorporated between the FGF2 terminus and ABD to minimize interference between the two domains during expression and binding events (Figure 2a). This methodology is advantageous versus disulfide bond immobilization for proteins that require cysteines for activity or cannot be modified to contain thiols.

FGF2 was immobilized with 3D control using the HSA and ABD physical interaction. After first immobilizing mal-HSA, we then introduced and immobilized FGF2-ABD-546 within the irradiated volumes. As shown for disulfide bond immobilization, the amount immobilized was dependent on the number of laser scans, although in this case, a higher concentration of protein was immobilized for the same number of scans when compared to that used for FGF2 immobilization using disulfide bonds. The increase is most likely a result of the immobilization procedure. For the disulfide bond method, the gels were patterned first followed by the introduction of FGF2. Therefore, some photodeprotected thiols in agarose may have reacted with other functional groups, such as forming disulfide bonds between agarose thiols in the patterned region. For the HSA/ABD method, mal-HSA was present at the time of patterning, which limited the formation of disulfide cross-links within the gel and increased the amount of free thiols for reaction. For both systems, the concentration of protein immobilized was linear with irradiation, indicating that only a fraction of thiols were used. This was expected because the gels have a thiol-Bhc concentration of 820 μM, which is much higher than the nanomolar range of the immobilized protein. Importantly, the axial resolution ($\sim$40 μm) remained the same between the two systems, which indicates that the resolution is solely dependent on the volume of excitation and not the immobilization strategy. Immobilization of proteins using the physical binding pair of HSA and ABD produces a stable complex. The presence of soluble HSA did not influence the FGF2-ABD pattern, indicating this method can be used under conditions that include albumin such as in vitro cell culture or even in vivo. If the FGF2-ABD complex with HSA was disassembling, the amount of immobilized protein would decrease faster in the samples stored in HSA solutions than in those stored in PBS. Soluble HSA would prevent reattachment of FGF2-ABD to agarose-immobilized HSA because it is at a much higher concentration. The similar changes in FGF2-ABD observed between samples stored in HSA and PBS indicate a very slow dissociation of the complex. This result is consistent with the reported dissociation rate constant of HSA/ABD ($k_D = 1.5 \times 10^{-6}$ s^{-1}),[31] which is similar to that of biotin-streptavidin ($K_D = 6.8 \times 10^{-5}$ s^{-1}).[42] An interaction with femtomolar dissociation constants and very low dissociation rate constants is commonly termed a "quasi-covalent interaction".[43]

The use of disulfide bonds or physical binding pairs with two-photon irradiation allows for 3D protein immobilization under mild conditions. Traditional 3D photopatterning techniques have relied on the use of chemical cross-linkers or photoinitiators, which can negatively influence bioactivity or cell viability. The methods described above allow for the immobilization of proteins in buffers without the use of potentially cytotoxic organic molecules. The use of binding domains also directs the site of immobilization on the protein molecule, which in turn can control protein orientation for optimal bioactivity. In this case, ABD was placed at the C-terminus, leaving the N-terminus of the protein free for receptor binding. For another protein, where the binding site is at the C-terminus, ABD could have been placed at the N-terminus, thereby leaving the C-terminus free. Thus, the molecular location of immobilization can be dialed in, depending on which protein region is needed for receptor binding. The ABD could have been placed at either terminus of FGF2, because neither the N-terminus nor the C-terminus is not involved in receptor binding (Protein Data Bank entry 1EV2).[44] Furthermore, immobilization using binding systems is versatile because it can be applied to any protein expressed as a fusion protein with ABD.

CONCLUSIONS

The ability to form 3D patterns of proteins within hydrogels provides a useful tool to the fields of cell biology where the 3D

microenvironment is known to influence cell fate. To this end, we have developed two separate techniques in which proteins were 3D patterned with the ability to vary immobilized concentrations. The disulfide bond system provides a direct immobilization method for proteins with free cysteines. This simple method requires only the native protein for immobilization and light and will thus facilitate 3D protein patterning for nonexperts within the fields of regenerative medicine. The HSA and ABD system provides a versatile immobilization method and can be applied to any protein because it is not dependent on any intrinsic property of the biologically relevant protein. The incorporation of ABD provides additional control over the orientation of the immobilized proteins. Furthermore, both systems provide immobilization methods without the need of cross-linking agents that could be detrimental to protein bioactivity or cell viability. These methods should have broad applicability in research involving biochemical patterning.

AUTHOR INFORMATION

Corresponding Author

*The Donnelly Centre, 160 College St., Room 514, Toronto, ON M5S 3E1. E-mail: molly.shoichet@utoronto.ca. Phone: (416) 978-1460. Fax: (416) 978-4317.

Notes

The authors declare no competing financial interests.

ACKNOWLEDGMENT

We are grateful to the Ontario Centres of Excellence (OCE) and the Natural Sciences and Engineering Research Council (NSERC) (M.S.S.) for partial funding of this research. We are also grateful to the Le Fonds Québécoise de la recherche sur la nature et les technologies (R.G.W.). We thank members of the Shoichet research laboratory for thoughtful discussions, particularly Drs. Michael Cooke and Shawn Owen.

REFERENCES

(1) Tibbitt, M. W.; Anseth, K. S. Hydrogels as extracellular matrix mimics for 3D cell culture. *Biotechnol. Bioeng.* **2009**, *103* (4), 655–663.

(2) Owen, S. C.; Shoichet, M. S. Design of three dimensional biomimetic scaffolds. *J. Biomed. Mater. Res., Part A* **2010**, *94* (4), 1321–1331.

(3) Kloxin, A. M.; Kloxin, C. J.; Bowman, C. N.; Anseth, K. S. Mechanical properties of cellularly responsive hydrogels and their experimental determination. *Adv. Mater.* **2010**, *22* (31), 3484–3494.

(4) Geckil, H.; Xu, F.; Zhang, X.; Moon, S. J.; Demirci, U. Engineering hydrogels as extracellular matrix mimics. *Nanomedicine* **2010**, *5* (3), 469–484.

(5) Luo, Y.; Shoichet, M. S. A photolabile hydrogel for guided three-dimensional cell growth and migration. *Nat. Mater.* **2004**, *3* (4), 249–253.

(6) DeForest, C. A.; Polizzotti, B. D.; Anseth, K. S. Sequential click reactions for synthesizing and patterning three-dimensional cell microenvironments. *Nat. Mater.* **2009**, *8* (8), 659–664.

(7) Aizawa, Y.; Wylie, R.; Shoichet, M. Endothelial cell guidance in 3-D patterned scaffolds. *Adv. Mater.* **2010**, *22*, 4831–4835.

(8) Hersel, U.; Dahmen, C.; Kessler, H. RGD modified polymers: Biomaterials for stimulated cell adhesion and beyond. *Biomaterials* **2003**, *24* (24), 4385–4415.

(9) Campbell, P. G.; Miller, E. D.; Fisher, G. W.; Walker, L. M.; Weiss, L. E. Engineered spatial patterns of FGF-2 immobilized on fibrin direct cell organization. *Biomaterials* **2005**, *26* (33), 6762–6770.

(10) Nur-E-Kamal, A.; Ahmed, I.; Kamal, J.; Babu, A. N.; Schindler, M.; Meiners, S. Covalently attached FGF-2 to three-dimensional polyamide nanofibrillar surfaces demonstrates enhanced biological stability and activity. *Mol. Cell. Biochem.* **2008**, *309* (1), 157–166.

(11) Hynes, R. O. The extracellular matrix: Not just pretty fibrils. *Science* **2009**, *326* (5957), 1216.

(12) Ito, T.; Sawada, R.; Fujiwara, Y.; Tsuchiya, T. FGF-2 increases osteogenic and chondrogenic differentiation potentials of human mesenchymal stem cells by inactivation of TGF- signaling. *Cytotechnology* **2008**, *56* (1), 1–7.

(13) Rabchevsky, A.; Fugaccia, I.; Turner, A.; Blades, D.; Mattson, M.; Scheff, S. Basic fibroblast growth factor (bFGF) enhances functional recovery following severe spinal cord injury to the rat. *Exp. Neurol.* **2000**, *164* (2), 280–291.

(14) Schultz, G. S.; Wysocki, A. Interactions between extracellular matrix and growth factors in wound healing. *Wound Repair and Regeneration* **2009**, *17* (2), 153–162.

(15) Montesano, R.; Vassalli, J. D.; Baird, A.; Guillemin, R.; Orci, L. Basic fibroblast growth factor induces angiogenesis in vitro. *Proc. Natl. Acad. Sci. U.S.A.* **1986**, *83* (19), 7297.

(16) Marra, K. G.; DeFail, A. J.; Clavijo-Alvarez, J. A.; Badylak, S. F.; Taieb, A.; Schipper, B.; Bennett, J.; Rubin, J. P. FGF-2 enhances vascularization for adipose tissue engineering. *Plast. Reconstr. Surg.* **2008**, *121* (4), 1153.

(17) Miller, E. D.; Fisher, G. W.; Weiss, L. E.; Walker, L. M.; Campbell, P. G. Dose-dependent cell growth in response to concentration modulated patterns of FGF-2 printed on fibrin. *Biomaterials* **2006**, *27* (10), 2213–2221.

(18) DeLong, S. A.; Moon, J. J.; West, J. L. Covalently immobilized gradients of bFGF on hydrogel scaffolds for directed cell migration. *Biomaterials* **2005**, *26* (16), 3227–3234.

(19) DeForest, C. A.; Sims, E. A.; Anseth, K. S. Peptide-Functionalized Click Hydrogels with Independently Tunable Mechanics and Chemical Functionality for 3D Cell Culture. *Chem. Mater.* **2010**, *22*, 4783–4790.

(20) Fairbanks, B. D.; Schwartz, M. P.; Halevi, A. E.; Nuttelman, C. R.; Bowman, C. N.; Anseth, K. S. A versatile synthetic extracellular matrix mimic via thiol-norbornene photopolymerization. *Adv. Mater.* **2009**, *21* (48), 5005–5010.

(21) Hahn, M. S.; Miller, J. S.; West, J. L. Three Dimensional Biochemical and Biomechanical Patterning of Hydrogels for Guiding Cell Behavior. *Adv. Mater.* **2006**, *18* (20), 2679–2684.

(22) Hoffmann, J. C.; West, J. L. Three-dimensional photolithographic patterning of multiple bioactive ligands in poly(ethylene glycol) hydrogels. *Soft Matter* **2010**, *6* (20), 5056–5063.

(23) Lee, S. H.; Moon, J. J.; West, J. L. Three-dimensional micropatterning of bioactive hydrogels via two-photon laser scanning photolithography for guided 3D cell migration. *Biomaterials* **2008**, *29* (20), 2962–2968.

(24) Leslie-Barbick, J. E.; Shen, C.; Chen, C.; West, J. L. Micron-scale spatially patterned, covalently immobilized vascular endothelial growth factor on hydrogels accelerates endothelial tubulogenesis and increases cellular angiogenic responses. *Tissue Eng., Part A* **2011**, *17* (1−2), 221–229.

(25) Saik, J. E.; Gould, D. J.; Keswani, A. H.; Dickinson, M. E.; West, J. L. Biomimetic hydrogels with immobilized EphrinA1 for therapeutic angiogenesis. *Biomacromolecules* **2011**, *12* (7), 2715–2722.

(26) Xu, C.; Webb, W. W. Measurement of two-photon excitation cross sections of molecular fluorophores with data from 690 to 1050 nm. *J. Opt. Soc. Am. B* **1996**, *13* (3), 481–491.

(27) Furuta, T.; Wang, S. S. H.; Dantzker, J. L.; Dore, T. M.; Bybee, W. J.; Callaway, E. M.; Denk, W.; Tsien, R. Y. Brominated 7-hydroxycoumarin-4-ylmethyls: Photolabile protecting groups with biologically useful cross-sections for two photon photolysis. *Proc. Natl. Acad. Sci. U.S.A.* **1999**, *96* (4), 1193.

(28) Rusmini, F.; Zhong, Z.; Feijen, J. Protein immobilization strategies for protein biochips. *Biomacromolecules* **2007**, *8* (6), 1775–1789.

(29) Zhang, K.; Diehl, M. R.; Tirrell, D. A. Artificial Polypeptide Scaffold for Protein Immobilization. *J. Am. Chem. Soc.* **2005**, *127* (29), 10136–10137.

(30) Wosnick, J. H.; Shoichet, M. S. Three-dimensional chemical patterning of transparent hydrogels. *Chem. Mater.* **2008**, *20* (1), 55–60.
(31) Jonsson, A.; Dogan, J.; Herne, N.; Abrahmsén, L.; Nygren, P. Å. Engineering of a femtomolar affinity binding protein to human serum albumin. *Protein Eng., Des. Sel.* **2008**, *21* (8), 515.
(32) Invitrogen. Amine reactive probes.
(33) Chiasson, B. J.; Tropepe, V.; Morshead, C. M.; van der Kooy, D. Adult mammalian forebrain ependymal and subependymal cells demonstrate proliferative potential, but only subependymal cells have neural stem cell characteristics. *J. Neurosci.* **1999**, *19* (11), 4462.
(34) Hermanson, G. T. *Bioconjugate techniques*; Academic Press: San Diego, 1996.
(35) Hein, K. L.; Kragh-Hansen, U.; Morth, J. P.; Jeppesen, M. D.; Otzen, D.; Møller, J. V.; Nissen, P. Crystallographic analysis reveals a unique lidocaine binding site on human serum albumin. *J. Struct. Biol.* **2010**, *171* (3), 353–360.
(36) Tognon, G.; Frapolli, R.; Zaffaroni, M.; Erba, E.; Zucchetti, M.; Faircloth, G. T.; D'Incalci, M. Fetal bovine serum, but not human serum, inhibits the in vitro cytotoxicity of ET-743 (Yondelis, trabectedin). *Cancer Chemother. Pharmacol.* **2004**, *53* (1), 89–90.
(37) Kang, C. E.; Tator, C. H.; Shoichet, M. S. Poly(ethylene glycol) modification enhances penetration of fibroblast growth factor 2 to injured spinal cord tissue from an intrathecal delivery system. *J. Controlled Release* **2010**, *144* (1), 25–31.
(38) Gasparian, M.; Elistratov, P.; Drize, N.; Nifontova, I.; Dolgikh, D.; Kirpichnikov, M. Overexpression in *Escherichia coli* and purification of human fibroblast growth factor (FGF-2). *Biochemistry (Moscow, Russ. Fed.)* **2009**, *74* (2), 221–225.
(39) McCall, M. J.; Diril, H.; Meares, C. F. Simplified method for conjugating macrocyclic bifunctional chelating agents to antibodies via 2-iminothiolane. *Bioconjugate Chem.* **1990**, *1* (3), 222–226.
(40) Parisot, J.; Kurz, K.; Hilbrig, F.; Freitag, R. Use of azobenzene amino acids as photo responsive conformational switches to regulate antibody−antigen interaction. *J. Sep. Sci.* **2009**, *32* (10), 1613–1624.
(41) Leipzig, N. D.; Wylie, R. G.; Kim, H.; Shoichet, M. S. Differentiation of neural stem cells in three-dimensional growth factor-immobilized chitosan hydrogel scaffolds. *Biomaterials* **2011**, *32* (1), 57–64.
(42) Chivers, C. E.; Crozat, E.; Chu, C.; Moy, V. T.; Sherratt, D. J.; Howarth, M. A streptavidin variant with slower biotin dissociation and increased mechanostability. *Nat. Methods* **2010**, *7* (5), 391.
(43) Nguyen, D.; Dhanasekaran, P.; Phillips, M. C.; Lund-Katz, S. Molecular Mechanism of Apolipoprotein E Binding to Lipoprotein Particles. *Biochemistry (Moscow, Russ. Fed.)* **2009**, *48* (13), 3025–3032.
(44) Plotnikov, A. N.; Hubbard, S. R.; Schlessinger, J.; Mohammadi, M. Crystal structures of two FGF-FGFR complexes reveal the determinants of ligand-receptor specificity. *Cell* **2000**, *101* (4), 413–424.